

A multi-objective optimization procedure to develop modified-embedded-atom-method potentials: an application to magnesium

J. Houze,^{1,2} Sungho Kim,^{1,2} Amitava Moitra,^{1,2} B. Jelinek,^{1,2} Sebastien Groh,^{2,3}
M. F. Horstemeyer,^{2,3} Erdem Acar,⁴ Masoud Rais-Rohani,⁴ and Seong-Gon Kim^{1,2,5,*}

¹Department of Physics and Astronomy, Mississippi State University, Mississippi State, MS 39762, USA

²Center for Advanced Vehicular Systems, Mississippi State University, Mississippi State, MS 39762, USA

³Department of Mechanical Engineering, Mississippi State University, Mississippi State, MS 39762, USA

⁴Department of Aerospace Engineering, Mississippi State University, Mississippi State, MS 39762, USA

⁵Center for Computational Sciences, Mississippi State University, Mississippi State, MS 39762, USA

(Dated: October 18, 2021)

We have developed a multi-objective optimization (MOO) procedure to construct modified-embedded-atom-method (MEAM) potentials with minimal manual fitting. This procedure has been applied successfully to develop a new MEAM potential for magnesium. The MOO procedure is designed to optimally reproduce multiple target values that consist of important materials properties obtained from experiments and first-principles calculations based on density-functional theory (DFT). The optimized target quantities include elastic constants, cohesive energies, surface energies, vacancy formation energies, and the forces on atoms in a variety of structures. The accuracy of the new potential is assessed by computing several material properties of Mg and comparing them with those obtained from other potentials previously published. We found that the present MEAM potential yields a significantly better overall agreement with DFT calculations and experiments.

PACS numbers: 34.20.Cf, 61.43.Bn, 61.72.Ji, 62.20.Dc, 68.35.-p

I. INTRODUCTION

Molecular dynamics simulations are effective tools used to study many interesting phenomena such as the melting and coalescence of nanoparticles at the atomic scale.^{1,2} These atomistic simulations require accurate interaction potentials to compute the total energy of the system, and first-principles calculations can provide the most reliable interatomic potentials. However, realistic molecular dynamics simulations often require an impractical number of atoms that either demands too much computer memory or takes too long to be completed in a reasonable amount of time. One alternative is to use empirical or semi-empirical interaction potentials that can be evaluated efficiently.

The modified-embedded-atom method (MEAM) proposed by Baskes et al.^{3,4,5} is one of the most widely used methods using semi-empirical atomic potentials to date. The MEAM is an extension of the embedded-atom method (EAM) to include angular forces.^{6,7,8} The MEAM and EAM use a single formalism to generate semi-empirical potentials that have been successfully applied to a large variety of materials including fcc, bcc, hcp, diamond-structured materials and even gaseous elements, to produce simulations in good agreement with experiments or first-principles calculations.^{3,4,5,8}

Despite its remarkable successes, one of the most notable difficulties in using MEAM is that the construction of the MEAM potentials involves a lot of manual and *ad hoc* fittings. Because of the complex relationship between the sixteen MEAM parameters and the resultant behavior of a MEAM potential, a traditional procedure for constructing a MEAM potential involves a two-step iterative process. First, a *single* crystal structure, designated as

the reference structure, is chosen and the MEAM parameters are fitted to construct a MEAM potential that reproduces a handful of critical materials properties of the element in the reference structure. Second, the new potential is tested for its accuracy and transferrability by applying it to atoms under circumstances not used during its construction phase. These systems include different crystal structures, surfaces, stacking faults, and point defects. If the validation is not satisfactory, one needs to go back to the first step and adjust the parameters in a way that improves the overall quality of the potential. Although this iterative method does work eventually in many cases, it is a very tedious and time-consuming. Ercolessi and Adams overcame this shortcoming for EAM potentials by developing a force-matching method that fits the EAM potential to *ab initio* atomic forces of many atomic configurations including surfaces, clusters, liquids and crystals at finite temperature.⁹ Later, the force-matching method was extended to include many other materials properties such as cohesive energy, lattice constants, stacking fault energies, and elastic constants.^{10,11} Furthermore, several different MEAM potentials for the same element often develop and an objective and quantitative method to measure the relative quality of each potential would be helpful for the researchers who want to choose one of these potentials.

In this work, we extend the force-matching method to develop a multi-objective optimization (MOO) procedure to construct MEAM potentials. Most realistic optimization problems, particularly in engineering, require the simultaneous optimization of more than one objective function. For example, aircraft design requires simultaneous optimization of fuel efficiency, payload and weight calls for a MOO procedure. In most cases, it

is unlikely that the different objectives would be optimized by the same parameter choices. Therefore, some trade-off between the objectives is needed to ensure a satisfactory design. Stadler¹² introduced the concept of Pareto optimality¹³ to the fields of engineering and science. The most widely used method for multi-objective optimization is the weighted sum method. A comprehensive overview and comparison of different MOO methods can be found in Ref. 14.

The composite objective function also provides an unbiased measure to quantify the relative quality of different MEAM potentials. We apply the procedure to develop a new MEAM potential for magnesium. The new Mg MEAM potential will be compared with previously published Mg potentials.

We chose Mg because of its increased importance in many technological areas, including the aerospace and automotive industries. Due to the lower mass densities of magnesium alloys compared with steel and aluminum and higher temperature capabilities and improved crash-worthiness than plastics, the use of magnesium die castings is increasing rapidly in the automotive industry.^{15,16,17}

Empirical potentials for Mg have been previously proposed by several groups. In 1988, Oh and Johnson developed analytical EAM potentials for hcp metals such as Mg.¹⁸ Igarashi, Kanta and Vitek¹⁹ (IKV) also developed interatomic potentials for eight hcp metals including Mg using the Finnis–Sinclair type many-body potentials.²⁰ Pasianot and Savino²¹ proposed improved EAM potentials for Mg based on IKV’s fitting scheme. Baskes and Johnson⁵ have extended the modified embedded atom method (MEAM)^{3,4,8} to hcp crystal structures. Later, Jelinek et al. improved this potential as a part of the MEAM potentials for Mg–Al alloy system.²² Liu et al. used the force-matching method to develop an EAM potential for Mg.¹⁰

The paper is organized in the following manner. In Sec. II, we give a brief review of the MEAM. In Sec. III, the procedure for determination of the MEAM parameters is presented in detail. In Sec. IV, we assess the accuracy and transferability of our MEAM potential and make comparisons to other previously published potentials.

II. METHODOLOGY

A. MEAM

The total energy E of a system of atoms in the MEAM²³ is approximated as the sum of the atomic energies

$$E = \sum_i E_i. \quad (1)$$

The energy of atom i consists of the embedding energy and the pair potential terms:

$$E_i = F_i(\bar{\rho}_i) + \frac{1}{2} \sum_{j \neq i} \phi_{ij}(r_{ij}). \quad (2)$$

F_i is the embedding function of atom i ; $\bar{\rho}_i$ is the background electron density at the site of atom i ; and $\phi_{ij}(r_{ij})$ is the pair potential between atoms i and j separated by a distance r_{ij} . The embedding energy $F_i(\bar{\rho}_i)$ represents the energy cost to insert atom i at a site where the background electron density is $\bar{\rho}_i$. The embedding energy is given in the form

$$F_i(\bar{\rho}_i) = A_i E_i^0 \bar{\rho}_i \ln(\bar{\rho}_i), \quad (3)$$

where the parameters E_i^0 and A_i depend on the element type of atom i . The background electron density $\bar{\rho}_i$ is given by

$$\bar{\rho}_i = \frac{\rho_i^{(0)}}{\rho_i^0} G(\Gamma_i), \quad (4)$$

where

$$\Gamma_i = \sum_{k=1}^3 \bar{t}_i^{(k)} \left(\frac{\rho_i^{(k)}}{\rho_i^{(0)}} \right)^2 \quad (5)$$

and

$$G(\Gamma) = \sqrt{1 + \Gamma}. \quad (6)$$

The zeroth and higher order densities, $\rho_i^{(0)}$, $\rho_i^{(1)}$, $\rho_i^{(2)}$, and $\rho_i^{(3)}$ are given in Eq. (9). The composition-dependent electron density scaling ρ_i^0 is given by

$$\rho_i^0 = \rho_{i0} Z_{i0} G(\Gamma_i^{\text{ref}}), \quad (7)$$

where ρ_{i0} is an element-dependent density scaling, Z_{i0} is the first nearest-neighbor coordination of the reference system, and Γ_i^{ref} is given by

$$\Gamma_i^{\text{ref}} = \frac{1}{Z_{i0}^2} \sum_{k=1}^3 \bar{t}_i^{(k)} s_i^{(k)}, \quad (8)$$

where $s_i^{(k)}$ is the shape factor that depends on the reference structure for atom i . Shape factors for various structures are specified in the work of Baskes⁴. The par-

tial electron densities are given by

$$\rho_i^{(0)} = \sum_{j \neq i} \rho_j^{a(0)} S_{ij} \quad (9a)$$

$$\left(\rho_i^{(1)}\right)^2 = \sum_{\alpha} \left[\sum_{j \neq i} \rho_j^{a(1)} \frac{r_{ij\alpha}}{r_{ij}} S_{ij} \right]^2 \quad (9b)$$

$$\left(\rho_i^{(2)}\right)^2 = \sum_{\alpha, \beta} \left[\sum_{j \neq i} \rho_j^{a(2)} \frac{r_{ij\alpha} r_{ij\beta}}{r_{ij}^2} S_{ij} \right]^2 - \frac{1}{3} \left[\sum_{j \neq i} \rho_j^{a(2)} S_{ij} \right]^2 \quad (9c)$$

$$\left(\rho_i^{(3)}\right)^2 = \sum_{\alpha, \beta, \gamma} \left[\sum_{j \neq i} \rho_j^{a(3)} \frac{r_{ij\alpha} r_{ij\beta} r_{ij\gamma}}{r_{ij}^3} S_{ij} \right]^2 - \frac{3}{5} \sum_{\alpha} \left[\sum_{j \neq i} \rho_j^{a(3)} \frac{r_{ij\alpha}}{r_{ij}} S_{ij} \right]^2, \quad (9d)$$

where $r_{ij\alpha}$ is the α component of the displacement vector from atom i to atom j . S_{ij} is the screening function between atoms i and j and is defined in Eqs. (16). The atomic electron densities are computed as

$$\rho_i^{a(k)}(r_{ij}) = \rho_{i0} \exp \left[-\beta_i^{(k)} \left(\frac{r_{ij}}{r_i^0} - 1 \right) \right], \quad (10)$$

where r_i^0 is the nearest-neighbor distance in the single-element reference structure and $\beta_i^{(k)}$ are element-dependent parameters. Finally, the average weighting factors are given by

$$\bar{t}_i^{(k)} = \frac{1}{\rho_i^{(0)}} \sum_{j \neq i} t_j^{(k)} \rho_j^{a(0)} S_{ij}, \quad (11)$$

where $t_j^{(k)}$ is an element-dependent parameter.

The pair potential is given by

$$\phi_{ij}(r_{ij}) = \bar{\phi}_{ij}(r_{ij}) S_{ij} \quad (12)$$

$$\bar{\phi}_{ij}(r_{ij}) = \frac{1}{Z_{ij}} \left[2E_{ij}^u(r_{ij}) - F_i \left(\frac{Z_{ij} \rho_j^{(0)}(r_{ij})}{Z_i \rho_i^0} \right) - F_j \left(\frac{Z_{ij} \rho_i^{(0)}(r_{ij})}{Z_j \rho_j^0} \right) \right] \quad (13)$$

$$E_{ij}^u(r_{ij}) = -E_{ij}^0 (1 + a_{ij}^*(r_{ij})) e^{-a_{ij}^*(r_{ij})} \quad (14)$$

$$a_{ij}^* = \alpha_{ij} \left(\frac{r_{ij}}{r_{ij}^0} - 1 \right), \quad (15)$$

where α_{ij} is an element-dependent parameter. The sublimation energy E_{ij}^0 , the equilibrium nearest-neighbor distance r_{ij}^0 , and the number of nearest-neighbors Z_{ij} are obtained from the reference structure.

The screening function S_{ij} is designed so that $S_{ij} = 1$ if atoms i and j are unscreened and within the cutoff radius r_c , $S_{ij} = 0$ if they are completely screened or outside the cutoff radius, and varies smoothly between 0 and 1 for partial screening. The total screening function is the product of a radial cutoff function and three-body terms involving all other atoms in the system:

$$S_{ij} = \bar{S}_{ij} f_c \left(\frac{r_c - r_{ij}}{\Delta r} \right) \quad (16a)$$

$$\bar{S}_{ij} = \prod_{k \neq i, j} S_{ikj} \quad (16b)$$

$$S_{ikj} = f_c \left(\frac{C_{ikj} - C_{\min, ikj}}{C_{\max, ikj} - C_{\min, ikj}} \right) \quad (16c)$$

$$C_{ikj} = 1 + 2 \frac{r_{ij}^2 r_{ik}^2 + r_{ij}^2 r_{jk}^2 - r_{ij}^4}{r_{ij}^4 - (r_{ik}^2 - r_{jk}^2)^2} \quad (16d)$$

$$f_c(x) = \begin{cases} 1 & x \geq 1 \\ [1 - (1 - x)^4]^2 & 0 < x < 1 \\ 0 & x \leq 0 \end{cases} \quad (16e)$$

Note that C_{\min} and C_{\max} can be defined separately for each i - j - k triplet, based on their element types. The parameter Δr controls the distance over which the radial cutoff function changes from 1 to 0 near $r = r_c$.

B. Multi-objective Optimization

A generic multi-objective optimization (MOO) problem can be formulated as^{24,25}:

$$\begin{aligned} \min \mathbf{J}(\mathbf{x}) \quad \text{s.t.} \quad & \mathbf{x} \in S \\ \text{where } \mathbf{J} = & [J_1(\mathbf{x}) \cdots J_m(\mathbf{x})]^T \\ \mathbf{x} = & [x_1 \cdots x_n]^T \end{aligned} \quad (17)$$

Here, \mathbf{J} is a column vector of m objectives, whereby $J_i \in \mathbb{R}$. The individual objectives are dependent on a vector \mathbf{x} of n design variables in the feasible domain S . The design variables are assumed to be continuous and vary independently. Typically, the feasible design domain is defined by the design constraints and the bounds on the design variables. The problem is to minimize all elements of the objective vector simultaneously. The most widely used method for MOO is scalarization using the weighted sum method. The method transforms the multiple objectives into an aggregated scalar objective function J that is the sum of each objective function J_i multiplied by a positive weighting factor w_i :

$$J(\mathbf{x}) = \sum_{i=1}^m w_i J_i(\mathbf{x}). \quad (18)$$

In this work, the overall goal is to develop a MEAM potential for Mg. The individual objective functions are

constructed from the normalized differences between the MEAM-generated values and the target values:

$$J_i(\mathbf{x}) = \left[\frac{Q_i(\mathbf{x}) - Q_i^0}{Q_i^*} \right]^2. \quad (19)$$

Here, Q_i is the physical quantity computed using the current MEAM potential parameters and Q_i^0 is the target value to reproduce. The target values are usually experimental values, but the computed values from the first-principles method are chosen when the experimental data are not available. The normalization factor Q_i^* is a typical value for the given materials parameter and often $Q_i^* = Q_i^0$. The overall objective function $J(\mathbf{x})$ can be minimized using usual multi-dimensional optimization routines. To avoid unnecessary complications, we used the *downhill simplex method*,²⁶ which requires only function evaluations, not derivatives.

III. POTENTIAL CONSTRUCTION PROCEDURE

We used the MOO procedure to develop a new set of MEAM parameters that improves the overall agreement of MEAM results with experiments or *ab initio* calculations. Our previously published MEAM parameters for Mg²² served as the basis for the present work.

All *ab initio* total-energy calculations and geometry optimizations are performed within density functional theory (DFT) using ultrasoft pseudopotentials (USPP)²⁷ as implemented by Kresse et. al.^{28,29} For the treatment of electron exchange and correlation, we use local-density approximation (LDA)^{30,31}. The Kohn-Sham equations are solved using a preconditioned band-by-band conjugate-gradient (CG) minimization.³² The plane-wave cutoff energy is set to at least 300 eV in all calculations. Geometry relaxations are performed until the energy difference between two successive ionic optimizations is less than 0.001 eV. The Brillouin zone is sampled using the Monkhorst-Pack scheme³³ and a Fermi-level smearing of 0.2 eV was applied using the Methfessel-Paxton method.³⁴

The objectives used in this work include equilibrium hcp lattice constants a and c at 0 K, the cohesive energy, elastic constants, vacancy formation energy, surface energies, stacking fault energies, and adsorption energies. We also used the forces on Mg atoms in structures equilibrated at six different temperatures. The final MEAM parameters obtained from the MOO procedure are listed in Table I. Table II shows the complete list of objectives optimized to construct the MEAM potential parameters for Mg and their weights.

1. Cohesive energies

The cohesive energy of Mg atom is defined as the heat of formation per atom when Mg atoms are assembled into

a crystal structure:

$$E_{\text{coh}} = \frac{E_{\text{tot}} - NE_{\text{atom}}}{N}, \quad (20)$$

where E_{tot} is the total energy of the system, N is the number of Mg atoms in the system, and E_{atom} is the total energy of an isolated Mg atom. The cohesive energies of Mg atoms in hcp, fcc, and bcc crystal structures for several atomic volumes near the equilibrium atomic volumes were calculated. Fig. 1 is an example of the cohesive energy plot of Mg atoms as a function of the lattice constant. The minimum of this curve determines the equilibrium lattice constant a_0 and equilibrium cohesive energies $E_{\text{hcp}} = E_{\text{hcp}}$ in Table II.

2. Elastic constants

Hexagonal crystals have five independent elastic constants: C_{11} , C_{12} , C_{13} , C_{33} , and C_{44} .³⁵ The elastic constants are calculated numerically by applying small strains to the lattice. For small deformations, the relationship between deformation strain and elastic energy increase in an hcp crystal is quadratic:¹⁰

1. $\Delta U = \delta^2(C_{11} + C_{12})$, for deformation $x' = x + \delta \cdot x$, $y' = y + \delta \cdot y$,
2. $\Delta U = \delta^2(C_{11} - C_{12})$, for deformation $x' = x + \delta \cdot x$, $y' = y - \delta \cdot y$,
3. $\Delta U = \delta^2 C_{33}/2$, for deformation $z' = z + \delta \cdot z$,
4. $\Delta U = \delta^2(2C_{11} + C_{33} + 2C_{12} + 4C_{13})/2$, for deformation $x' = x + \delta \cdot x$, $y' = y + \delta \cdot y$, $z' = z + \delta \cdot z$,
5. $\Delta U = \delta^2 C_{44}/2$, for deformation $z' = z + \delta \cdot x$,

where unprimed (primed) are the coordinates of the lattice before (after) deformation. ΔU is the elastic energy due to the deformation, and δ is the small strain applied to the lattice. We follow the procedure described by Mehl et al.³⁶ and apply several different strains ranging from -2.0% to $+2.0\%$. The elastic constants are obtained by fitting the resultant curves to quadratic functions. We found that this method gives much more stable results than using one strain value¹⁰.

3. Surface formation energies

Surface formation energy per unit surface area is defined as

$$\gamma = (E_{\text{tot}} - N\varepsilon)/A, \quad (21)$$

where E_{tot} is the total energy of the system with a surface, N is the number of atoms in the system, ε is the total energy per atom in the bulk, and A is the surface area. Table II lists the surface formation energies

used in this study. The (10 $\bar{1}$ 0) surface of hcp crystals can be terminated in two ways, either with a short first interlayer distance d_{12} (“short termination”) or with a long d_{12} (“long termination”) (See, for example, Fig. 2 of Ref. 37). In this study, we only included the results for the short terminated surface, since it is known to be energetically more favorable over the long terminated surface³⁸ in agreement with experimental observations in Be(10 $\bar{1}$ 0) and other hcp metals.³⁷

4. Stacking fault energies

Stacking fault formation energy per unit area is defined by

$$E_{\text{sf}} = (E_{\text{tot}} - N\varepsilon) / A, \quad (22)$$

where E_{tot} is the total energy of the structure with a stacking fault, N is the number of atoms in the system, ε is the total energy per atom in the bulk, and A is the unit cell area that is perpendicular to the stacking fault. For Mg, four stacking fault types from the calculation of Chetty et al.³⁹ were examined. The sequences of the atomic layers within the unit cell of our simulations are: $I_1 = ABABABCBCBCB$, $I_2 = ABABABCACACB$, $T_2 = ABABABCABAB$, and $E = ABABABCABAB$. We note that the unit cells for I_1 and I_2 contain *two* stacking faults and the quantities obtained from Eq. (22) must be divided by two to obtain the correct formation energies.

5. Vacancy formation energies

The formation energy of a single vacancy E_{vac} is defined as the energy cost to create a vacancy:

$$E_{\text{vac}} = E_{\text{tot}}[N] - N\varepsilon, \quad (23)$$

where $E_{\text{tot}}[N]$ is the total energy of a system with N atoms containing a vacancy, and ε is the energy per atom in the bulk.

6. Atomic Forces

For forces, the objective functions are defined as:

$$J_i(\mathbf{x}) = \frac{\langle\langle(\mathbf{F} - \mathbf{F}^0)^2\rangle\rangle^{1/2}}{\langle\langle(\mathbf{F}^0)^2\rangle\rangle^{1/2}}, \quad (24)$$

where \mathbf{F} are the force vectors on atoms calculated using the MEAM while \mathbf{F}^0 are the force vectors from DFT method. $\langle\langle(\mathbf{F}^0)^2\rangle\rangle^{1/2}$ represents the root-mean-square of the DFT force, and $\langle\langle(\mathbf{F} - \mathbf{F}^0)^2\rangle\rangle^{1/2}$ is the root-mean-square of the error in the force.

To obtain the force data, initial atomic structures that contain 180 Mg atoms were created from the bulk hcp

crystal structure. The positions of atoms are randomly disturbed from their equilibrium positions and 10 000 steps of molecular-dynamics (MD) simulations with a timestep of $\Delta t = 2.5$ ps were performed to equilibrate each structure for different temperatures. In each MD run, we used Mg MEAM potential by Jelinek et al.²² If no MEAM potential were available for MD simulations, one could use an intermediate MEAM potential that is generated with this MOO procedure without the force data. The potential should be adequate enough to obtain a reasonable set of structures.

IV. RESULTS AND DISCUSSION

The hcp structure was chosen as the reference structure for Mg. The final MEAM parameters obtained from the MOO procedure are listed in Table I.

A. Materials properties

Table II lists various materials properties of Mg selected as the objectives to be optimized in constructing Mg MEAM potential, along with experimental data and *ab initio* data. It also shows how well each objective has been optimized. Results from other previously published Mg potentials are also listed in the table for comparison. Table II also shows the weight of individual objectives w_i chosen to optimize the present potential. The underlined quantities are the target values chosen for the MOO procedure. Whenever possible, the experimental values are chosen as the target values. If the experimental values are not available or known to be unreliable, the computed values from the first-principles method are used.

The present MEAM potential reproduces the experimental lattice constant, the c/a ratio, and the cohesive energy near perfectly. Fig. 1 shows the cohesive energies of Mg atoms in hcp crystal structure compared with those obtained from the Rose universal equation of state⁴⁶ based on the experimental lattice constant, cohesive energy and bulk modulus. It shows a good agreement between the two sets of data. We also note that the sequence of the structures is predicted correctly in the order of stability by the present Mg MEAM potential as shown in Table II.

The surface formation energies of the two common low-index surfaces of hcp Mg crystals are in good agreement with the experimental values, representing a significant improvement over the previously published MEAM potentials.^{22,47,48}

As pointed out by Liu et al.¹⁰, the stacking fault energies are difficult quantities for an empirical potential to reproduce because they only depend on long range interactions beyond second nearest-neighbor distances in hcp crystals. The present MEAM potential shows a substantial improvement over the previously published MEAM potential by Hu et al.⁴⁵ The stacking fault energies are

TABLE I: Set of the MEAM potential parameters for Mg. See Sec. II A for the definition of these parameters and their usage. The hcp structure was chosen as the reference structure for Mg.

E^0 [eV]	a_0 [Å]	A	α	$\beta^{(0)}$	$\beta^{(1)}$	$\beta^{(2)}$	$\beta^{(3)}$	$t^{(0)}$	$t^{(1)}$	$t^{(2)}$	$t^{(3)}$	C_{\max}	C_{\min}	r_c	Δr
1.51	3.20	1.14	5.69	2.66	-0.003	0.348	3.32	1.00	8.07	4.16	-2.02	3.22	1.10	5.0	0.353

TABLE II: The objectives optimized to construct the MEAM potential parameters for Mg along with the target values and their weights. Comparisons to other Mg potentials are also made. E_{coh} is the cohesive energy, B is the bulk modulus, γ is the surface energy, E_{sf} is the stacking fault formation energy, E_{vac} is the relaxed vacancy formation energy, and $\Delta\mathbf{F}$ is the relative error in forces. The underlined quantities are the target values chosen for the MOO procedure.

	Objective	Unit	Weight	Expt	DFT	MEAM ^a	Jelinek ^b	Liu ^c	Hu ^d
1	a_0	Å	1.0	<u>3.21</u> [40]	3.128	3.21	3.21	3.21	
2	c/a	-	1.0	<u>1.623</u> [40]	1.623	1.622	1.623	1.623	
3	$E_{\text{coh}} = E_{\text{hcp}}$	eV	2.0	<u>1.51</u> [41]	1.78	1.51	1.55	1.52	
4	B	kbar	1.0	<u>369</u> [42]		376	353	367	
5	$E_{\text{fcc}} - E_{\text{hcp}}$	meV	0.72		<u>14</u> [43]	4	4	15	
6	$E_{\text{bcc}} - E_{\text{hcp}}$	meV	0.72		<u>29</u> [43]	34	30	18	
7	C_{11}	kbar	1.0	<u>635</u> [42]		606	602	618	
8	C_{12}	kbar	1.0	<u>260</u> [42]		274	237	259	
9	C_{13}	kbar	1.0	<u>217</u> [42]		250	219	219	
10	C_{33}	kbar	1.0	<u>665</u> [42]		631	623	675	
11	C_{44}	kbar	1.0	<u>184</u> [42]		151	155	182	
12	$\gamma[(0001)]$	mJ/m ²	1.0	680 [44]	<u>637</u>	583	595	495	310
13	$\gamma[(10\bar{1}0)]$	mJ/m ²	1.0		<u>721</u>	625	645		
14	$E_{\text{sf}}[I_1]$	eV	0.1		<u>18</u>	8	7	27	4
15	$E_{\text{sf}}[I_2]$	eV	0.1		<u>37</u>	15	15	54	8
16	$E_{\text{sf}}[T_2]$	eV	0.1		<u>45</u>	15	15		
17	$E_{\text{sf}}[E]$	eV	0.1		<u>61</u>	23	22		12
28	E_{vac}	eV	1.0	0.58 ~ 0.89	<u>0.82</u>	0.58	0.56	0.87	0.59
19	$\Delta\mathbf{F}$ (100 K)	%	1.0		<u>0.0</u>	38.13	201.51		
20	$\Delta\mathbf{F}$ (300 K)	%	1.0		<u>0.0</u>	29.67	93.73		
21	$\Delta\mathbf{F}$ (500 K)	%	1.0		<u>0.0</u>	25.18	59.17		
22	$\Delta\mathbf{F}$ (800 K)	%	1.0		<u>0.0</u>	25.08	98.77		
23	$\Delta\mathbf{F}$ (1000 K)	%	1.0		<u>0.0</u>	26.93	85.31		
24	$\Delta\mathbf{F}$ (1200 K)	%	1.0		<u>0.0</u>	27.30	79.77		

^aMEAM potential from the present work

^bMEAM potential from Ref. 22

^cEAM potential from Ref. 10

^dAnalytic MEAM potential from Ref. 45

consistently underestimated by the present MEAM potential compared to the results of the DFT calculations, while the results by the EAM potential from Ref. 10 are consistently overestimated. Table II also shows that the formation energy of single vacancies from DFT calculation is reproduced quite reasonably by the present MEAM potential.

Table II also shows the force-matching against the *ab initio* forces database. It shows that the MEAM potential from the present work reproduces more accurate forces on atoms compared to the previous MEAM potential²².

B. Additional materials properties

To validate the present MEAM potential further, we calculated a few additional materials properties of Mg

TABLE III: The additional materials properties of Mg that are not used as objectives for the construction of the potential. Comparisons are made to other Mg potentials and experiments. E_{ads} is the adsorption energy; $E_{\text{f}}^{\text{int}}$ is the formation energies of interstitial point defects. All energy values are given in eV.

Property	DFT	MEAM ^a	Jelinek ^b
$E_{\text{ads}}[(0001)]$	-0.81	-1.46	-1.50
$E_{\text{ads}}[(10\bar{1}0)]$	-1.21	-1.52	-1.56
$E_{\text{f}}^{\text{int}}$ (octahedral)	2.36	1.20	1.29
$E_{\text{f}}^{\text{int}}$ (tetrahedral)	2.35	1.41	1.53

^aMEAM potential from the present work

^bMEAM potential from Ref. 22

that were not used as objectives during the construction of the potential. We obtained the adsorption energies of

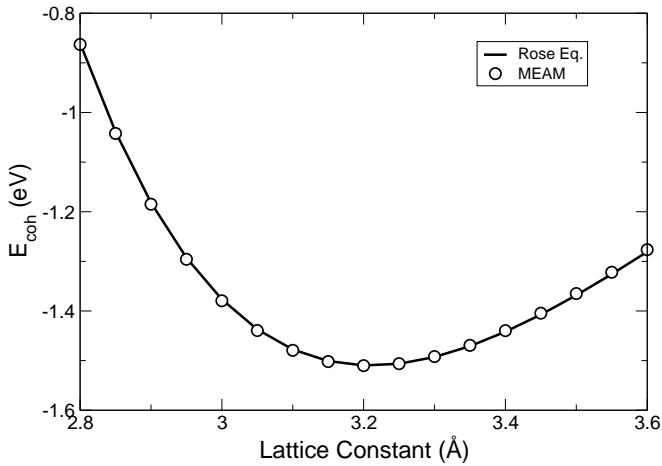


FIG. 1: The cohesive energies as a function of the lattice constant a for Mg atoms in hcp crystal structure compared with the ones obtained from the Rose equation. The data points are computed with the present MEAM potential while the curve is obtained from the Rose equation.

a single Mg atom on different surfaces and the formation energies of interstitial defects as listed in Table III.

The adsorption energy of a single adatom E_{ads} is given by

$$E_{\text{ads}} = E_{\text{tot}} - E_{\text{surf}} - E_{\text{atom}}, \quad (25)$$

where E_{tot} is the total energy of the structure with the adatom adsorbed on the surface, E_{surf} is the total energy of the surface without the adatom, and E_{atom} is the total energy of an isolated atom. On both (0001) and (10 $\bar{1}$ 0) surfaces, we placed a single Mg atom at the site where the atoms of the next layer would normally sit. The structures were then relaxed to determine the adsorption energies. Table III shows that the adsorption energies on two Mg surfaces are quite well reproduced by the present MEAM potential. The present Mg potential gives slightly better adsorption energies than the previously published MEAM potential²².

The formation energy of an interstitial point defect $E_{\text{f}}^{\text{int}}$ is given by

$$E_{\text{f}}^{\text{int}} = E_{\text{tot}}[N + 1] - (E_{\text{tot}}[N] + \varepsilon), \quad (26)$$

where $E_{\text{tot}}[N]$ is the total energy of a system with N Mg atoms, $E_{\text{tot}}[N + 1]$ is the total energy of a system with N atoms plus one Mg atom inserted at one of the interstitial sites, and ε is the total energy per Mg atom in its most stable bulk structure. Interstitial atom formation energies were calculated for Mg at octahedral and tetrahedral sites. Atomic position and volume relaxation were performed. The results of these calculations are listed in Table III, to be compared with the results from the DFT calculations. The present MEAM potential predicts correct signs for these energies although the magnitudes are about half of those predicted by DFT. MEAM potentials predict that the octahedral site will be more stable than

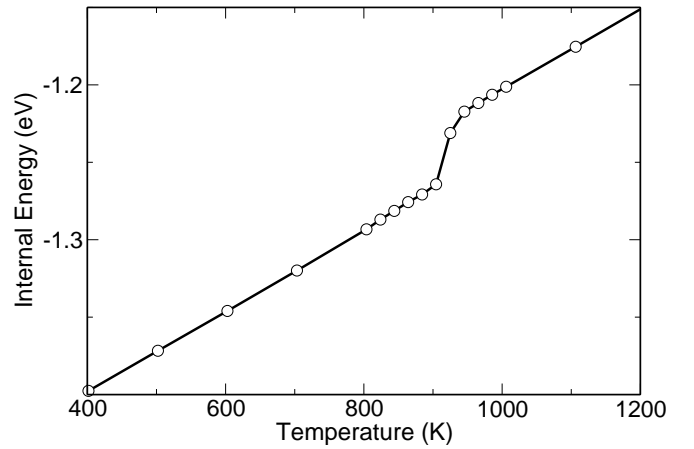


FIG. 2: The internal energies of Mg crystal in hcp structure as a function of temperature. The energies are obtained from the ensemble average of the MD simulations of five structures containing 448 Mg atoms.

the tetrahedral site, while the DFT calculations indicate that both sites will have nearly the same formation energies.

C. Thermal properties

To validate the new potential for molecular dynamics simulations, we calculated the melting temperatures of pure Mg crystals. We followed a single-phase method as described by Kim and Tománek,² in which the temperature is increased at a constant rate and the internal energy of the system is monitored. Fig. 2 shows the internal energies of Mg crystal in hcp structure as a function of temperature. The plot was obtained from the ensemble average of five hcp structures containing 448 Mg atoms. The initial velocity vectors were set randomly according to the Maxwell-Boltzmann velocity distribution at $T = 100$ K. The temperature of the system was controlled by using a Nosé-Hoover thermostat.^{49,50} It is clearly seen from Fig. 2 that the internal energy curve makes an abrupt transition from one linear region to another, marking the melting point. Using this method, we obtained 920 K as the melting temperature of Mg crystals. This result is in good agreement with the experimental value of 923 K. Our result represents a substantial improvement in accuracy from 745 K obtained from a previously published EAM potential¹⁰ or 780 K from a MEAM potential.²²

V. CONCLUSIONS

In this study, we developed a multi-objective optimization procedure to construct MEAM potentials with minimal manual fitting. We successfully applied this procedure to develop a set of MEAM parameters for Mg in-

teratomic potential based on first-principles calculations within DFT. The validity and transferability of the new MEAM potentials were tested rigorously by calculating the physical properties of the Mg systems in many different atomic arrangements such as bulk, surface, point defect structures, and molecular dynamics simulations. The new MEAM potential shows a significant improvement over previously published potentials, especially for the atomic forces and melting temperature calculations.

VI. ACKNOWLEDGMENT

This work has been supported in part by the US Department of Energy under Grant No. DE-AC05-00OR22725 subcontract No. 4000054701. Computer time allocation has been provided by the High Performance Computing Collaboratory (HPC²) at Mississippi State University.

-
- * Electronic address: kimg@ccs.msstate.edu
- ¹ S. J.-H., L. B.-J., and C. Y.W., Surf. Sci. **512**, 262 (2002).
 - ² S. G. Kim and D. Tománek, Phys. Rev. Lett. **72**, 2418 (1994).
 - ³ M. I. Baskes, J. S. Nelson, and A. F. Wright, Phys. Rev. B **40**, 6085 (1989).
 - ⁴ M. I. Baskes, Phys. Rev. B **46**, 2727 (1992).
 - ⁵ M. I. Baskes and R. A. Johnson, Modell. Simul. Mater. Sci. Eng. **2**, 147 (1994).
 - ⁶ M. S. Daw and M. I. Baskes, Phys. Rev. Lett. **50**, 1285 (1983).
 - ⁷ M. S. Daw and M. I. Baskes, Phys. Rev. B **29**, 6443 (1984).
 - ⁸ M. I. Baskes, Phys. Rev. Lett. **59**, 2666 (1987).
 - ⁹ F. Ercolessi and J. Adams, Europhys. Lett. **26**, 583 (1994).
 - ¹⁰ X.-Y. Liu et al., Modell. Simul. Mater. Sci. Eng. **4**, 004 (1996).
 - ¹¹ Y. Li et al., Phys. Rev. B **67**, 125101 (2003).
 - ¹² S. W., J. of Optimization Theory and Applications **29**, 1 (1979).
 - ¹³ V. Pareto, *Manuale di Economia Politica* (Societa Editrice Libreria, 1909), translated into English by A.S. Schwier as *Manual of Political Economy*, Macmillan, New York, 1971.
 - ¹⁴ J. Andersson, Ph.D. thesis, Linköping University, Linköping, Sweden (2001).
 - ¹⁵ Q. Han, K. B. K., and V. Srinath, Philos. Mag. **84**, 3843 (2005).
 - ¹⁶ A. Lou, J. Renaud, I. Nakatsugawa, and J. Plourde, JOM **47**, 28 (1995).
 - ¹⁷ G. Pettersen, H. Westergen, R. Hoier, and L. O., Mater. Sci. Eng. A **207**, 115 (1996).
 - ¹⁸ D. J. Oh and R. A. Johnson, J. Mater. Res. **3**, 471 (1988).
 - ¹⁹ M. Igarashi, M. Khantha, and V. Vitek, Philos. Mag. B **63**, 603 (1991).
 - ²⁰ M. Finnis and J. Sinclair, Philos. Mag. A **50**, 45 (1984).
 - ²¹ R. Pasianot and E. J. Savino, Phys. Rev. B **45**, 12704 (1992).
 - ²² B. Jelinek et al., Phys. Rev. B **75**, 054106 (pages 9) (2007).
 - ²³ Y.-M. Kim, B.-J. Lee, and M. I. Baskes, Phys. Rev. B **74**, 014101 (pages 12) (2006).
 - ²⁴ I. Y. Kim and O. L. de Weck, Structural and Multidisciplinary Optimization **31**, 105 (2005).
 - ²⁵ *Multiojective Optimization: History and Promise* (The Third China-Japan-Korea Joint Symposium on Optimization of Structural and Mechanical Systems, Kanazawa, Japan, 2004).
 - ²⁶ W. H. Press, B. P. Flannery, S. A. Teukolsky, and W. T. Vetterling, *Numerical Recipes in C: The Art of Scientific Computing* (Cambridge University Press, Cambridge, 1992), 2nd ed.
 - ²⁷ D. Vanderbilt, Phys. Rev. B **41**, 7892 (1990).
 - ²⁸ G. Kresse and J. Hafner, J. Phys.: Cond. Matt. **6**, 8245 (1994).
 - ²⁹ G. Kresse and J. Furthmüller, Phys. Rev. B **54**, 11169 (1996).
 - ³⁰ D. M. Ceperley and B. J. Alder, Phys. Rev. Lett. **45**, 566 (1980).
 - ³¹ J. P. Perdew and A. Zunger, Phys. Rev. B **23**, 5048 (1981).
 - ³² G. Kresse and J. Hafner, Phys. Rev. B **47**, 558 (1993).
 - ³³ H. J. Monkhorst and J. D. Pack, Phys. Rev. B **13**, 5188 (1976).
 - ³⁴ M. Methfessel and A. T. Paxton, Phys. Rev. B **40**, 3616 (1989).
 - ³⁵ H. M. Ledbetter, Journal of Physical and Chemical Reference Data **6**, 1181 (1977).
 - ³⁶ M. J. Mehl, B. M. Klein, and D. A. Papaconstantopoulos, in *Intermetallic Compounds: Principles and Applications*, edited by J. H. Westbrook and R. L. Fleischer (John Wiley & Sons Ltd., London, 1994).
 - ³⁷ P. Hofmann, K. Pohl, R. Stumpf, and E. W. Plummer, Phys. Rev. B **53**, 13715 (1996).
 - ³⁸ P. Staikov and T. S. Rahman, Phys. Rev. B **60**, 15613 (1999).
 - ³⁹ N. Chetty and M. Weinert, Phys. Rev. B **56**, 10844 (1997).
 - ⁴⁰ J. Emsley, *The Elements* (Oxford University Press, Oxford, UK, 1998), 3rd ed.
 - ⁴¹ C. Kittel, *Introduction to Solid State Physics* (John Wiley & Sons, Inc., Hoboken, NJ, 1996), 7th ed.
 - ⁴² C. J. Smith, ed., *Metal Reference Book* (Butterworth, London, UK, 1976), 5th ed.
 - ⁴³ J. D. Althoff et al., Phys. Rev. B **48**, 13253 (1993).
 - ⁴⁴ W. R. Tyson and W. A. Miller, Surf. Sci. **62**, 267 (1977).
 - ⁴⁵ W. Hu, B. Zhang, B. Huang, F. Gao, and D. J. Bacon, J. Phys.: Condens. Matter **13**, 1193 (2001).
 - ⁴⁶ J. H. Rose, J. R. Smith, F. Guinea, and J. Ferrante, Phys. Rev. B **29**, 2963 (1984).
 - ⁴⁷ B.-J. Lee, J.-H. Shim, and M. I. Baskes, Phys. Rev. B **68**, 144112 (2003).
 - ⁴⁸ W. Hu, H. Deng, X. Yuan, and M. Fukumoto, Eur. Phys. J. B **34**, 429 (2003).
 - ⁴⁹ S. Nosé, J. Chem. Phys. **81**, 511 (1984).
 - ⁵⁰ W. G. Hoover, Phys. Rev. A **31**, 1695 (1985).